

Slope of forward elastic π^+p scattering from 4.4 to 6.0 GeV/c

C. A. Rey, J. A. Poirier, A. J. Lennox,* and V. Srinivasan
 Department of Physics, University of Notre Dame, Notre Dame, Indiana 46556[†]

W. F. Baker, D. P. Eartly, S. M. Pruss, and A. A. Wehmann
 Fermi National Accelerator Laboratory, Batavia, Illinois 60510[‡]
 (Received 24 June 1976)

Angular distributions for $\pi^+p \rightarrow \pi^+p$ were measured for 13 incident-pion momenta from 4.4 to 6.0 GeV/c and for $-t$ less than ~ 0.1 (GeV/c)². This experiment was performed at the Zero Gradient Synchrotron of Argonne National Laboratory, where a focusing magnetic spectrometer and a scintillation-counter hodoscope were used. In fitting the angular distributions the strong-interaction contribution was parameterized by an exponential form $\exp(bt)$; the Coulomb interference was also included. The resulting values of the slope parameter for $|t| < \sim 0.1$ (GeV/c)² are presented for each incident beam momentum.

INTRODUCTION

Elastic scattering of pions by protons in the near-forward region has been the subject of study in many experiments. The differential cross sections measured in the forward direction are frequently fitted by a quadratic form

$$\frac{d\sigma}{dt} = \left(\frac{d\sigma}{dt}\right)_{t=0} \exp(bt + ct^2)$$

or a linear form with $c=0$. Forward scattering has been studied over a wide range of energies, although only a few measurements¹⁻⁹ are found in the momentum interval from 4 to 7 GeV/c.

In our experiment, we have obtained data at small momentum transfers for 13 incident momenta from 4.4 to 6.0 GeV/c and have measured the slope parameter for each of these momenta. The Coulomb interaction has been taken into account in fitting $d\sigma/dt$. The results of such fits are presented along with the contribution of the strong interaction alone.

APPARATUS

The beam of pions required for the experiment was produced at the Zero Gradient Synchrotron (ZGS) of Argonne National Laboratory. A layout of the apparatus used to obtain differential cross sections in the near forward direction is shown in Fig. 1. This apparatus is more fully described in a report on a simultaneous experiment which measured backward π^+p elastic scattering.¹⁰ The incident beam had a momentum spread of $\pm 1\%$; pions were identified by Čerenkov counters C1 and C2 and scintillation counters B1 through B5. Another Čerenkov counter (not shown) was used to veto positrons.

The beam pions impinged on a 25.4-cm-long liquid hydrogen target located in the gap of a C magnet which was used to calibrate the spectrometer

system but which was turned off during normal data taking. Those pions which scattered upward in the vertical plane entered a narrow scintillation counter, ϕ (22 cm high and 1.4 cm wide), and a counter hodoscope, θ_{HOD} . This hodoscope divided the vertical plane into five segments θ_1 through θ_5 , each 3.1 cm high, and covered laboratory scattering angles from 1.6° to 4.3°. Data from additional counters at smaller angles were not used because of contamination from multiple Coulomb scattering of the beam.

The momenta of the particles were measured by a focusing spectrometer which consisted of two quadrupole magnets and a dipole magnet with a 20-cm vertical gap. The first quadrupole magnet downstream of the hydrogen target was vertically focusing in order to obtain a large vertical acceptance. The second quadrupole was horizontally focusing. The dipole magnet was located between the two quadrupoles and bent the particles 9° in the

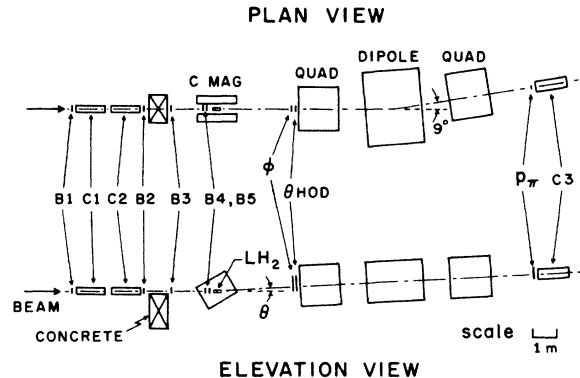


FIG. 1. Experimental layout. A ϕ counter, 1.4 cm in width, was used to define the scattering plane of this experiment. A 2.54-cm-wide counter just downstream of this ϕ counter was used in the backward π^+p elastic-scattering experiment, Ref. 10.

horizontal plane. A scintillation counter, p_π (1.27 cm wide and 18.1 cm high), was located at the final image formed by the focusing spectrometer for forward elastically scattered pions. Pions produced in inelastic interactions were kinematically excluded by the momentum constraint provided by this counter. The 30-cm-diameter, 91-cm-long Cerenkov counter, C3, was placed immediately after p_π and was used in coincidence to identify the pion. A coincidence between counters B1 through B5, C1, C2, ϕ , θ_{HOD} , p_π , and C3 could be satisfied either by an elastic π^+p scattering, by accidentals, or by scattering from matter other than the liquid hydrogen. The latter two backgrounds were corrected for by subtracting the target-empty data from the target-full data.

DATA TAKING

Conventional logic circuitry was used to measure the event rates for each hodoscope counter. These rates were recorded on scalers and were read into an on-line computer which also monitored the equipment. Data at each momentum setting were taken in several runs alternating between target full and target empty.

DATA REDUCTION

In order to extract the cross section, it was necessary to determine the acceptance of the spectrometer and the overall counter efficiencies. The C magnet was used to experimentally determine the spectrometer acceptance by deflecting the beam into each of the θ hodoscope counters and recording the fraction reaching the p_π counter. The spectrometer acceptance was $\geq 99\%$ for all but the last two counters and was 97% for $\theta 4$ and $\sim 20\%$ for $\theta 5$.

A computer program, TURTLE,¹¹ generated beam particles with the phase-space distribution of the actual beam and orbited them through the experimental setup with appropriate apertures. The spectrometer acceptance calculated from TURTLE agreed well with the experimental values, including the low acceptance for counter $\theta 5$. Because of the low efficiency of counter $\theta 5$, the data from this counter were not used in the final analysis.

For scattered pions, deviations from 100% acceptance were due in part to the finite width of the p_π counter (1.27 cm) and the shape of the final image. This effect was experimentally studied by varying the current in the B4 dipole magnet which swept the beam image across the p_π counter. These data are shown by dots in Fig. 2 as a function of $\Delta p/p$. The curve in the figure is the prediction from TURTLE.

The efficiency of the C3 Cerenkov counter was

70% because it did not accept the full pion image. The overall counter efficiency was observed to be independent of the scattering angle and hence of the momentum transfer. The t dependence of the measured cross sections was found to be independent of the momentum width of the incident beam. This was determined by taking some of the data at two different momentum widths.

The angular distributions are presented as a function of t in Fig. 3 for each of the 13 incident momenta. The errors shown are statistical only. In taking data at different momenta, none of the apparatus was moved and only the magnet currents were changed. Thus we estimate that the systematic errors are small compared to the statistical errors.

ANALYSIS

The data were analyzed by assuming that the total scattering amplitude can be expressed as

$$f_{\text{tot}} = f_s + f_c$$

where f_s and f_c are the complex strong-interaction and Coulomb-interaction amplitudes, respectively.

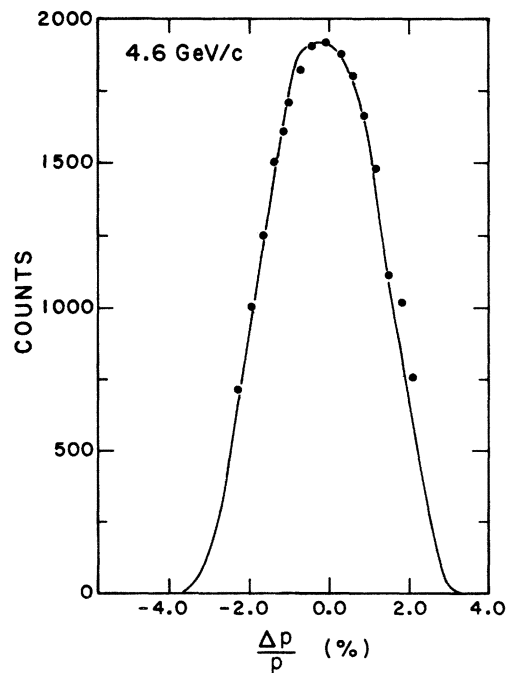


FIG. 2. The counting rate of pions in the p_π counter as a function of $\Delta p/p$ (%) at incident momentum 4.6 GeV/c. The dots are data and the curve is the prediction from a Monte Carlo program.

The differential cross section then becomes

$$\frac{d\sigma}{dt} = |f_s + f_c|^2 = |f_s|^2 + |f_c|^2 + 2 \operatorname{Re}(f_s^* f_c).$$

This can be written in terms of cross sections as

$$\begin{aligned} \frac{d\sigma}{dt} &= \left(\frac{d\sigma}{dt}\right)_s + \left(\frac{d\sigma}{dt}\right)_c \\ &\quad - 2 \left[\left(\frac{d\sigma}{dt}\right)_s \left(\frac{d\sigma}{dt}\right)_c \right]^{1/2} \frac{\rho \cos\delta + \sin\delta}{(1+\rho^2)^{1/2}}, \end{aligned}$$

where ρ is the ratio of the real part, f_R , to the imaginary part, f_I , of the strong amplitude. The values for ρ ranged from -0.30 to -0.27 over our momentum interval.¹² The Coulomb cross section is given¹³ by

$$\left(\frac{d\sigma}{dt}\right)_c = |f_c|^2,$$

where

$$f_c = \frac{-2\sqrt{\pi} \hbar c}{137t} \frac{\exp(i\delta)}{(1+t/0.71)^4},$$

where t is expressed in $(\text{GeV}/c)^2$ and δ is the phase shift between the Coulomb and the strong amplitudes; we have used

$$\delta = -[\ln(56.4t) + 0.5772]/137.$$

Over our t region the interference term contributes noticeably to the differential cross section though the Coulomb term by itself is negligible ($< 0.3\%$). The strong amplitude is parameterized by an exponential

$$\left(\frac{d\sigma}{dt}\right)_s = \left(\frac{d\sigma}{dt}\right)_{t=0} \exp(bt),$$

where b is the slope parameter for the strong interaction.

Standard least-square fitting methods were employed to obtain the fits presented by solid lines in Fig. 3. The dashed curves were obtained from these fits by subtracting out the Coulomb contribution, and can be interpreted as the effects of pure strong interactions. The slope parameter, b , is the slope of the dashed lines. We have normalized the data so that the ordinate for the dashed curve is 1.0 at $t=0$.

The fitted values for b from this experiment are given in Table I and are plotted in Fig. 4. The error bars indicate only the statistical errors; the

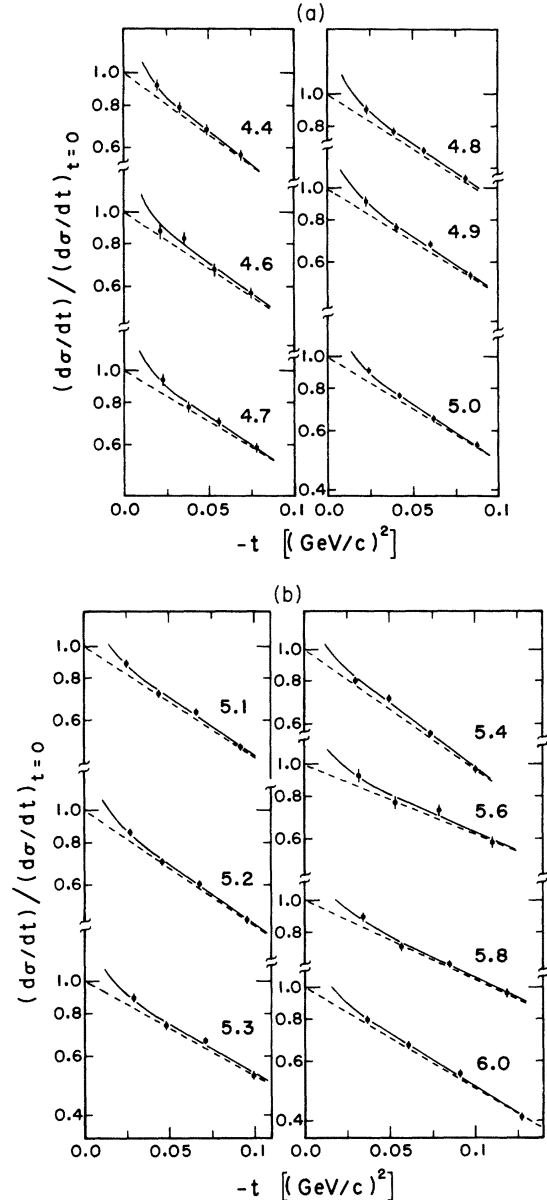


FIG. 3. The angular distribution for π^+p elastic scattering for each momentum given as a function of the momentum transfer squared, t . The solid lines are fits to the data including the Coulomb interaction. The dashed curves are results from the previous fit without the Coulomb-interaction contribution and represent the strong-interaction slope. Errors shown are statistical only.

systematic errors, which are not included, are small by comparison. The values of b found in other experiments are also presented in Fig. 4. Some experimenters with data over a larger t range fit their data with an additional quadratic term in t , namely $\exp(bt + ct^2)$. Because of the small t range of this experiment, our values for b are

only slightly affected by including this quadratic term. Small horizontal bars on the points of Fig. 4 indicate the values of b obtained by refitting both our data and data from other experiments with the inclusion of a quadratic term³ with $c = 2.24 \text{ (GeV/c)}^{-4}$.

We note the presence of apparent structure in the slope parameter around 5.7 GeV/c . The lower slopes obtained for the 5.6- and 5.8-GeV/c points are apparent in each of the separate runs at those momenta. The 5.6- and 5.8-GeV/c runs were separated by data taking at five lower momenta. Lasinski *et al.*⁹ have suggested that structure observed in the momentum dependence of the slope parameter is associated with the presence of Δ^{++} s -channel resonances, especially at incident beam momenta below $\sim 2 \text{ GeV/c}$. The apparent structure in our data cannot be explained by the presence of any of the established Δ^{++} resonances.

ACKNOWLEDGMENTS

We wish to thank Dr. Peter Koehler, Dr. K. P. Pretzl, and Dr. O. R. Sander for extensive help in all phases of this experiment. We wish to thank Dr. David Thomas, Venitios Polychronakos, and George Theodosiou for their help during the data-

TABLE I. Slope of the forward peak, b , in π^+p elastic scattering.

$p \text{ (GeV/c)}$	$b \pm \delta b \text{ [(GeV/c)}^{-2}\text{]}$
4.4	8.4 ± 1.0
4.6	7.6 ± 1.2
4.7	6.9 ± 0.8
4.8	7.2 ± 0.6
4.9	7.0 ± 0.7
5.0	7.1 ± 0.4
5.1	7.5 ± 0.5
5.2	7.8 ± 0.4
5.3	6.6 ± 0.5
5.4	8.0 ± 0.4
5.6	4.8 ± 0.7
5.8	5.5 ± 0.4
6.0	6.9 ± 0.4

taking phase, Dr. David Carey for software assistance, and Ron Erichsen, Cordon Kerns, William Rickhoff, and Hoshang Vaid for their technical assistance. It is a pleasure to thank the entire staff at the Argonne ZGS for advice and help throughout this experiment, and the University of Notre Dame Computing Center for aid in the data-analysis phase.

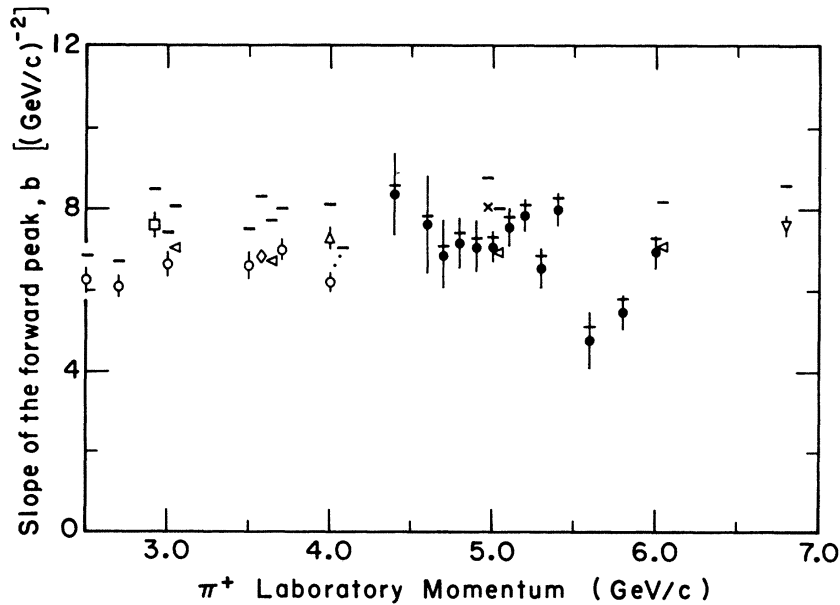


FIG. 4. Slope of the forward peak, b , given for each incident-pion momentum. ●: our data; □: Perl *et al.* (Ref. 2); ▽: Foley *et al.* (Ref. 3); △: Aderholz *et al.* (Ref. 4); ○: Coffin *et al.* (Ref. 5); ×: Rust *et al.* (Ref. 6); ◇: MacNaughton *et al.* (Ref. 7); ◁: Ambats *et al.* (Ref. 8). The horizontal bars indicate the value of b if a quadratic term in t is included with the coefficient $c = 2.24 \text{ (GeV/c)}^{-4}$ as obtained in Ref. 3.

*Present address: Fermi National Accelerator Laboratory, Batavia, Illinois 60510.

[†]Work supported in part by the National Science Foundation.

[‡]Work supported by the U. S. Energy Research and Development Administration.

¹Particle Data Group, LBL Report No. 63, 1973 (unpublished), p. 15; and Landolt-Börnstein, *Numerical Data and Functional Relationships in Science and Technology* (Springer, Berlin, 1973), Group I, Vol. 7.

²M. L. Perl, L. W. Jones, and C. C. Ting, Phys. Rev. 132, 1252 (1963).

³K. J. Foley, S. J. Lindenbaum, W. A. Love, S. Ozaki, J. J. Russell, and L. C. L. Yuan, Phys. Rev. Lett. 11, 425 (1963). Foley *et al.* have used an $\exp(bt + ct^2)$ form and found $b = 8.58 \pm 0.23$ (GeV/c)⁻² and $c = 2.24 \pm 0.29$ (GeV/c)⁻⁴ at 6.8 GeV/c.

⁴M. Aderholz, L. Bondar, M. Deutschmann, H. Lengeler, C. Thoma, H. Kaufmann, U. Kundt, K. Lanius, R. Leiste, R. Pose, D. C. Colley, W. P. Dodd, B. Musgrave, J. Simmons, K. Böckmann, G. Winter, V. Blobel, H. Butenschön, P. Von Handel, G. Wolf, E. Lohrmann, J. M. Brownlee, I. Butterworth, F. Campayne, M. Ibbotson, M. Saeed, N. N. Biswas, N. Schmitz, J. Weigl, and G. P. Wolf, Phys. Lett. 10, 248 (1964).

⁵C. T. Coffin, N. Dikman, L. Ettliger, D. Meyer,

A. Saulys, K. Terwilliger, and D. Williams, Phys. Rev. 159, 1169 (1967). We have fitted these data to a form $\exp(bt)$ over the first eight t values of each incident momentum; this limits the largest t value to the range -0.21 to -0.32 (GeV/c)².

⁶D. R. Rust, P. N. Kirk, R. A. Lundy, C. E. W. Ward, D. D. Yovanovitch, S. M. Pruss, C. W. Akerlof, K. S. Han, D. I. Meyer, and P. Schmueser, Phys. Rev. Lett. 24, 1361 (1970).

⁷J. MacNaughton, W. R. Butler, D. G. Coyne, G. M. Hicks, and G. H. Trilling, Nucl. Phys. B33, 101 (1971).

⁸T. Ambats, D. S. Ayres, R. Diebold, A. F. Greene, S. L. Kramer, A. Lesnik, D. R. Rust, C. E. W. Ward, A. B. Wicklund, and D. D. Yovanovitch, Phys. Rev. D 9, 1179 (1974).

⁹T. Lasinski, R. Levi Setti, and E. Predazzi, Phys. Rev. 179, 1426 (1969).

¹⁰A. J. Lennox, J. A. Poirier, C. A. Rey, O. R. Sander, W. F. Baker, D. P. Eartly, K. P. Pretzl, S. M. Pruss, A. A. Wehmann, and P. Koehler, Phys. Rev. D 11, 1777 (1975). The data for the present subsidiary experiment were taken concurrently with the data presented in this reference.

¹¹D. C. Carey, Nucl. Instrum. Methods 104, 173 (1972).

¹²G. Höhler and H. P. Jakob, Karlsruhe University Report No. TKP 23/72, 1972 (unpublished).

¹³M. P. Locher, Nucl. Phys. B2, 525 (1967).